

Color production in the Pati-Salam model

Sekazi K. Mtingwa and Murat Özer

Department of Physics and Astronomy, University of Maryland, College Park, Maryland 20742

(Received 12 May 1980)

We study the nucleon structure function F_2 for deep-inelastic scattering of leptons on an isoscalar target. The Owens-Reya parton distributions with charm added give good agreement with the data up to $Q^2 \sim 100$ GeV for the case of no color production. If color is produced, we describe in detail what effect this would have on F_2 to leading nontrivial order in Pati-Salam quantum chromodynamics with massive gluons.

The structure functions for electroproduction (muoproduction) processes in the $SU(4)_{\text{flavor}} \times SU(4)_{\text{color}}$ unified gauge theory of Pati and Salam,¹ involving integrally charged quarks and massive gluons, have been discussed by Özer and Pati.² The structure functions can be decomposed as follows:

$$F_i(Q^2, x) = F_i^{\text{flavor}}(Q^2, x) + F_i^{\text{color}}(Q^2, x)\theta(W - M_{\text{color}}), \quad (1)$$

where F_i^{flavor} corresponds to the usual quantum-chromodynamics (QCD) result for the production of color-singlet hadronic states, F_i^{color} corresponds to the production of color-nonsinglet states, and M_{color} is the invariant mass of the lightest color-octet hadronic final state transforming as $(8, 8)$ under $SU(3)_{\text{flavor}} \times SU(3)_{\text{color}}$. Of course, there are scalar partons in the Pati-Salam theory; however, Craigie and Salam³ have shown that if scalar-parton distributions are taken to be zero for small Q^2 and are generated dynamically at larger Q^2 values, then F_i^{flavor} should be indistinguishable from the conventional QCD result. Since their effect would be small, we neglect scalar partons below.

In the massive-gluon Pati-Salam model, color states are produced through exchanges of both the photon and its orthogonal color gauge partner \tilde{U} .⁴ Since the two contributions add with equal and opposite strengths, except that the photon is massless and the \tilde{U} has mass m_U , one gets a damping factor $\Delta^2 = [m_U^2 / (q^2 - m_U^2)]^2$ in F_1^{color} and F_2^{color} . The result in the simple parton model is that for $Q^2 \gtrsim 1-2$ GeV², one gets the following simple expressions for the nucleon color structure functions:

$$F_1^{\text{color}} \approx 0, \quad (2a)$$

$$F_2^{\text{color}} \approx \frac{1}{3} x v(x) \rho_{\text{color}}^{\text{th}}(Q^2, W^2), \quad (2b)$$

where $v(x)$ denotes the momentum distribution function for any one of the octet of gluons within the nucleon, and $\rho_{\text{color}}^{\text{th}}$ is the scale-threshold factor signifying that scaling (up to logarithmic corrections) is not realized until W is several GeV above

M_{color} . We use the form employed in Ref. 2:

$$\rho_{\text{color}}^{\text{th}}(Q^2, W^2) |_{Q^2 > 1 \text{ GeV}^2} = \theta(W - M_{\text{color}}) [1 - (M_{\text{color}}/W)^2]^\alpha. \quad (3)$$

We always choose the exponent α so that $\rho_{\text{color}}^{\text{th}}$ acquires a 75% saturation as W increases from M_{color} to $M_{\text{color}} + 2$ GeV.

Note in Eq. (2b) that the main increase in F_2 due to color production comes from the gluon partons and not from quark or scalar partons. And since the gluons reside at low- x values, one would expect color production to be a characteristically low- x phenomenon.

The quark momentum distributions are important to describe F_2^{flavor} . For this purpose we use the Buras-Gaemers valence-quark parametrizations⁵ and the Owens-Reya sea and gluon parametrizations.⁶ We further add the charmed sea as described below. One defines $u \equiv u_v + \xi$, $d \equiv d_v + \xi$, and $\bar{u} \approx \bar{d} \approx s \approx \bar{s} \equiv \xi$, where the subscripts v denote valence-quark distributions and ξ denotes the sea. The Buras-Gaemers valence-quark distributions are

$$x u_v(x, Q^2) + x d_v(x, Q^2) = \frac{3}{B(\eta_1, 1 + \eta_2)} x^{\eta_1} (1-x)^{\eta_2}, \quad (4a)$$

$$x d_v(x, Q^2) = \frac{1}{B(\eta_3, 1 + \eta_4)} x^{\eta_3} (1-x)^{\eta_4}, \quad (4b)$$

with

$$\begin{aligned} \eta_1 &= 0.70 - 0.176s, & \eta_2 &= 2.60 + 0.80s, \\ \eta_3 &= 0.85 - 0.24s, & \eta_4 &= 3.35 + 0.816s, \end{aligned} \quad (5)$$

where $s = \ln[\ln(Q^2/\Lambda^2)/\ln(Q_0^2/\Lambda^2)]$, $Q_0^2 = 1.8$ GeV², $\Lambda = 0.5$ GeV, and $B(\eta_i, 1 + \eta_{i+1})$ is the Euler beta function which ensures baryon-number conservation for all values of Q^2 . The Owens-Reya sea and gluon distributions are written in the form

$$\begin{aligned} x \xi(x, Q^2) &= A_s (1-x)^{\eta_s} + A'_s (1-x)^{\eta'_s} \\ &+ B_s e^{-C_s x}, \end{aligned} \quad (6a)$$

$$\begin{aligned} x G(x, Q^2) &= A_g (1-x)^{\eta_g} + A'_g (1-x)^{\eta'_g} \\ &+ B_g e^{-C_g x}, \end{aligned} \quad (6b)$$

where the coefficients and exponents are written as polynomials in s . The coefficients inside these polynomials in s are too numerous to enumerate here but they are given in Ref. 6.

Using the above parametrizations, about 6% of the parent nucleon's momentum is unaccounted for. We can reduce this to 1 or 2% by including the Buras-Gaemers charmed sea⁵ $C = c + \bar{c} = 2c$:

$$x C(x, Q^2) = \langle C(Q^2) \rangle_2 \left(\frac{\langle C(Q^2) \rangle_2}{\langle C(Q^2) \rangle_3} - 1 \right) \times (1-x)^{\langle C(Q^2) \rangle_2 / \langle C(Q^2) \rangle_3 - 2}, \quad (7)$$

where $\langle C(Q^2) \rangle_n \equiv \int_0^1 dx x^{n-1} C(x, Q^2)$, $n \geq 2$, is the charm quark's n th moment which we calculate from the Owens-Reya strange-quark distribution using the well-known QCD formula⁷

$$\langle c(Q^2) \rangle_n - \langle s(Q^2) \rangle_n = [\langle c(Q_0^2) \rangle_n - \langle s(Q_0^2) \rangle_n] \exp[-d_{NS}^n s], \quad (8)$$

with d_{NS}^n being proportional to the anomalous dimension of the spin- n nonsinglet operator. We take $\langle c(Q_0^2) \rangle_n = 0$.

We show in Fig. 1 that, aside from several suspiciously low data points, the above parton distributions give good agreement with the proton F_2^p structure function at $x=0.10$ as measured by Gordon *et al.*⁸ over a large range of Q^2 . Further, the above parton parametrizations give a good fit to the Gordon *et al.* data over a large range of x , and particularly over the range $x \lesssim 0.3$ of importance to this study. For example, Gordon *et al.*⁸ fit their full F_2^p data over the ranges $0 \leq x \leq 0.7$ and $1 \leq Q^2 \leq 65 \text{ GeV}^2$ with a phenomenological formula. We show in Fig. 2 how well the above parton parametrizations agree with their phenomenological formula for $x = 0.30$. The difference between the two curves is less than the error in the data.

So far, we have just concerned ourselves with parton distributions necessary to describe F_2^{1av} . To include the possibility of color production, we

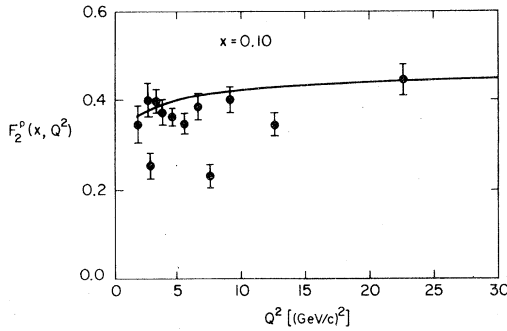


FIG. 1. Proton structure function F_2 vs Q_2 at $x=0.10$ together with data points from Gordon *et al.* (see Ref. 8).

need the leading-order quantum-chromodynamics (QCD) correction to Eq. (2b); therefore, we must solve the Altarelli-Parisi evolution equations⁹ for $G(x, Q^2) = 8v(x, Q^2)$ both below and above the color threshold Q_{th}^2 for fixed x . Below color threshold, $G(x, Q^2)$ evolves according to the conventional QCD formalism³; however, above color threshold, the evolution of $G(x, Q^2)$ is governed by the new P_{Gq} and P_{GG} calculated in Ref. 10:

$$P_{Gq}(z) = \frac{1-z}{6}, \quad (9a)$$

$$P_{GG}(z) = \frac{1}{32} \left(\frac{3}{2} \frac{1}{z^3} - \frac{1}{z^2} - 1 \right). \quad (9b)$$

To solve these evolution equations, let us follow the procedure of Feynman, Field, and Ross¹¹ and first define

$$A \otimes B \equiv \int_x^1 \frac{dz}{z} A\left(\frac{x}{z}\right) B(z). \quad (10)$$

Then we can write the Altarelli-Parisi evolution equations for the parton distributions above color threshold as follows:

$$\frac{d}{d\kappa} \begin{bmatrix} \Sigma(x, Q^2) \\ G(x, Q^2) \end{bmatrix} = \begin{bmatrix} P_{qq} & 2n_f P_{qG} \\ P_{Gq} & P_{GG} \end{bmatrix} \otimes \begin{bmatrix} \Sigma(z, Q^2) \\ G(z, Q^2) \end{bmatrix}, \quad (11)$$

where the P_{ab} are given in Ref. 10 [the relevant ones for this work being given in Eqs. (9a) and (9b)], Σ is the total quark distribution summed over all flavors, n_f is the number of quark flavors which we take to be four, and

$$\kappa = \frac{2}{(11 - \frac{2}{3}n_f)} \ln \left[\frac{\ln(Q^2/\Lambda^2)}{\ln(Q_{th}^2/\Lambda^2)} \right]. \quad (12)$$

Equation (11) can be written symbolically as

$$\frac{d}{d\kappa} \vec{G}(x, Q^2) = \vec{P} \otimes \vec{G}(z, Q^2), \quad (13)$$

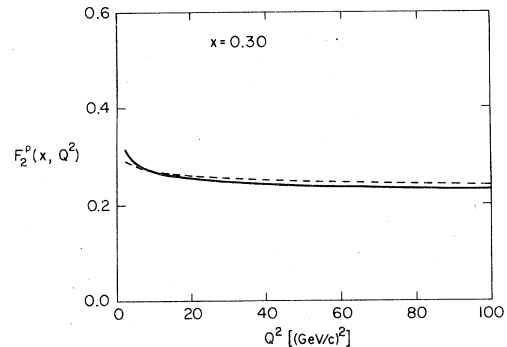


FIG. 2. Comparison of F_2^p at $x=0.30$ as given by the parametrizations in the text (solid line) and by the phenomenological formula of Gordon *et al.* (see Ref. 8).

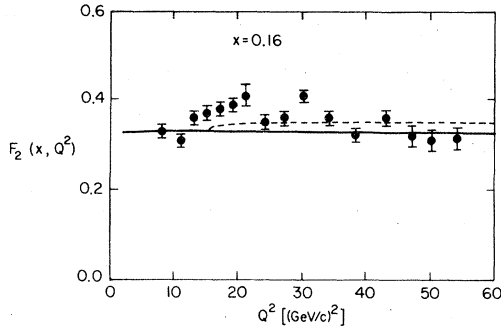


FIG. 3. F_2 per nucleon for an isoscalar target at $x=0.16$ and assuming $M_{\text{col}}=9$ GeV. The solid curve is the usual QCD result and the dashed curve includes the contribution from F_2^{col} . The data points are from Ball *et al.* (see Ref. 12).

with an obvious notation. Then the solution to Eq. (13) can be written

$$\vec{G}(x, Q^2) = \exp(\kappa \vec{P} \otimes) \vec{G}(Q_{\text{th}}^2). \quad (14)$$

We only need the gluon part of the solution since mainly the gluon distribution $v(x, Q^2) = \frac{1}{8} G(x, Q^2)$ contributes to F_2^{col} . One must also keep in mind that Eq. (14) is applicable only for $Q^2 \geq Q_{\text{th}}^2$ and that the boundary condition for Eq. (13) is chosen so that $G(x, Q^2)$ from the evolution below color threshold just matches that from Eq. (14) at $Q^2 = Q_{\text{th}}^2$.

After expanding Eq. (14) in κ and evaluating the integrals numerically, we find that for our purposes it is sufficient to retain only the leading and order- κ terms. We find that the term of order κ typically varies from between 0 to 1% of the leading term for $Q_{\text{th}}^2 \leq Q^2 \leq 100$ GeV².

In Fig. 3, we graph F_2 for an isoscalar-nucleon target at $x=0.16$ and assuming $M_{\text{col}}=9$ GeV. The data points are taken from Ball *et al.*¹² Note that the Pati-Salam theory with our parton parametrizations does not agree with the large increase of F_2 reported by Ball *et al.* We find that this is generally true for other values of x as well. In addition, we do not predict as large an increase in F_2 for color excitation as does Lehman.¹³ It is important to note that the anomalously large data points of Ball *et al.* have been reanalyzed by Ball¹⁴ and lowered to values more in line with the conventional QCD prediction.

We show in Figs. 4(a)–4(c) the percentage increase in F_2 above the conventional QCD prediction for an isoscalar nucleon target due to color production in the Pati-Salam model with the parton parametrizations discussed above. We examine the values $M_{\text{col}}=9, 11, 15,$ and 20 GeV at $x=0.05, 0.10,$ and 0.20 .

Color production in deep-inelastic scattering

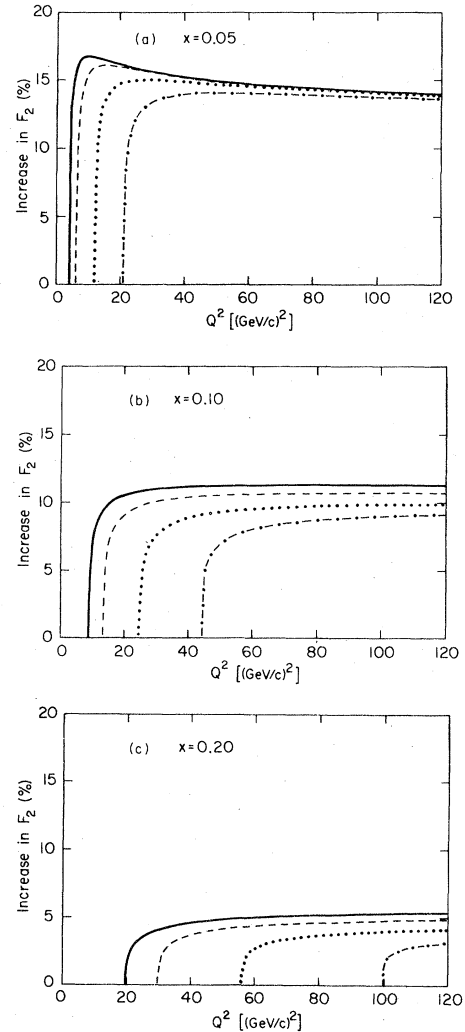


FIG. 4. (a)–(c) Percentage increase in F_2 above the conventional QCD prediction for $x=0.05, 0.10,$ and $0.20,$ respectively, and $M_{\text{col}}=9$ (solid line), 11 (dashed line), 15 (dotted line), and 20 (dash-dotted line) GeV.

may not be ruled out at the present time. Certainly our theoretical results do not agree with the data of Ball *et al.* for $M_{\text{col}}=9$ GeV; however, we have set up the theoretical machinery and made predictions for $M_{\text{col}} > 9$ GeV. One problem in trying to observe color production is that, aside from very small values of $x \lesssim 0.05$, the increase in F_2 due to color production may be less than the experimental errors and thus may be lost in the noise. We note that the Berkeley-Fermilab-Princeton Collaboration and the European Muon Collaboration¹⁵ have not seen the F_2 enhancement of Ball *et al.*¹² However, a word of caution is that neither of these two more recent collaborations smoothly spans the region 1 to 2 GeV² $\leq Q^2 \leq 20$ GeV² for $x \lesssim 0.05$, where we predict color

production would most noticeably manifest itself. Nonetheless, experimental techniques should be further refined in order to lay to rest this controversy over whether color can be seen in deep-inelastic scattering.

It is a pleasure to acknowledge stimulating discussions with Professor J. Pati, Professor S.

Oneda, and Professor A. Buras. Also, we are grateful to Professor R. Hartung for making Ball's thesis available to us. This work has been supported in part by the Center for Theoretical Physics, University of Maryland, the National Science Foundation, and the Computer Science Center, University of Maryland.

¹J. Pati and A. Salam, Phys. Rev. D 8, 1240 (1973); 10, 275 (1974).

²M. Özer and J. Pati, Nucl. Phys. B159, 293 (1979).

³N. Craigie and A. Salam, Phys. Lett. 85B, 57 (1979).

⁴J. Pati and A. Salam, Phys. Rev. Lett. 36, 11 (1976); G. Rajasekharan and P. Roy, Pramana 5, 303 (1975); Phys. Rev. Lett. 36, 355 (1976).

⁵A. Buras and K. Gaemers, Nucl. Phys. B132, 249 (1978).

⁶J. Owens and E. Reya, Phys. Rev. D 17, 3003 (1978).

⁷For an excellent discussion of Eq. (8) and QCD in general, see A. Buras, Rev. Mod. Phys. 52, 199 (1980).

⁸B. Gordon *et al.*, Phys. Rev. D 20, 2645 (1979).

⁹G. Altarelli and G. Parisi, Nucl. Phys. B126, 298 (1977).

¹⁰S. Mtingwa, Phys. Lett. 92B, 171 (1980).

¹¹For a discussion of this procedure, see R. Field, Report No. Calt-68-739, 1979 (unpublished).

¹²R. Ball *et al.*, Phys. Rev. Lett. 42, 866 (1979).

¹³E. Lehman, Phys. Rev. Lett. 42, 869 (1979).

¹⁴R. Ball, Ph.D. thesis, Michigan State University, 1979 (unpublished).

¹⁵For a discussion of these experiments, see E. Gaba-thuler, in *Proceedings of the International Conference on High-Energy Physics*, edited by A. Zichichi (CERN, Geneva, Switzerland, 1979), p. 697.